Journal of the Korean Nuclear Society
Volume 25, Number 1, March 1993

Evaluation of Axial Buckling Effect in On-Line Axial Power Shape Synthesis

Wang Kee In, Joon Sung Kim, Tae Young Yoon, Geun Sun Auh, and Hee Cheol Kim

Korea Atomic Energy Research Institute

(Received October 8, 1992)

실시간 노심출력분포 합성에서의 축방향 경계조건 영향평가

인왕기 · 김준성 · 윤태영 · 어근선 · 김희철

한국원자력연구소

(1992. 10. 8 접수)

Abstract

A fifth-order Fourier series technique is applied in Core Operating Limit Supervisory System (COLSS) to construct the on-line core average axial power shape from in-core detector signals because of its simplicity and fast computation. Such a synthesizing accuracy depends on number of Fourier series modes and axial boundary conditions. COLSS currently uses the five-mode Fourier series technique which utilizes the five axially located fixed in-core detector signals and a constant axial boundary condition. Therefore, the constant axial boundary condition should be appropriately chosen based on the evaluation of its effect on the accuracy of the on-line calculations. The four cases of axial buckling (0.75, 0.8, 0.9 and 1.0) were examined for Yonggwang Nuclear Units 3&4 as the axial boundary conditions in this paper. The core average axial power shapes and the operating margins were compared for each case to determine the optimal constant axial buckling. The axial buckling of 0.9 was found to be the optimal value.

요 약

노내계측기 신호로부터 노심평균 축방향 출력분포를 얻기위해 5차의 Fourier series 합성법이 노심감시계통 (COLSS)에 이용되고 있다. 이 방법은 단순하고 계산이 빠르기 때문에 실시간 계산에 이용된다. 이러한 합성법은 Fourier series 차수 및 축방향 경계조건에 따라 정확도가 달라진다. 노심감시계통에서는 현재 축방향으로 5개의 고정 노내계측기를 이용하고 있으므로 5차의 Fourier series 합성법을 적용하고 있다. 따라서 축방향 경계조건은 노심감시계통의 계산결과에 미치는 영향을 평가하여 적절히 결정되어야 한다. 본 논문에서는 영광 3,4호기를 대상으로 4가지의 축방향 경계조건 (axial buckling=0.75, 0.8, 0.9와 1.0)을 살펴보았다. 최적의 축방향 경계조건을 결정하기 위해 노심평균 축방향 출력분포와 운전여유도를 각 경우에 대해 비교하였다. 비교결과 최적의 축방향 경계조건은 axial buckling이 0.9인 것을 알 수 있었다.

1. Introduction

The Fourier series technique [1] has been widely applied to fit the data measured at finite locations. The fifth-order Fourier series technique is currently applied to the on-line synthesis of core average axial power shape in Core Operating Limit Supervisory System (COLSS) [2]. COLSS (Fig.1) is a digital computer based on-line monitoring system that is designed to assist the operator in monitoring of the Limiting Conditions for Operation (LCO). COLSS uses in-core detector signals and other plant measurements to monitor the nuclear power plant status, i.e., plant power, core average axial power shape and the margins to the LCO limits [3].

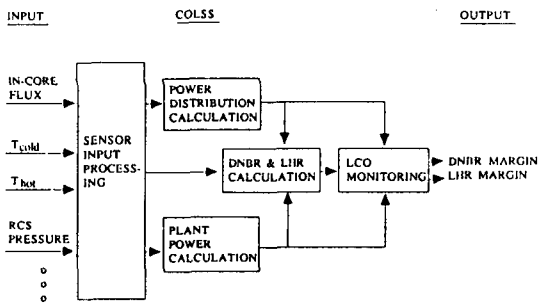

Fig. 1. Functional Block Diagram of COLSS

The Fourier series technique constructs the core average axial power shape from the in-core detector signals which is utilized in the on-line calculations of margins to both Linear Heat Rate (LHR) alarm and Departure from Nucleate Boiling Ratio (DNBR) alarm. The accuracy of Fourier series technique depends on the number of modes and the axial boundary condition. Since COLSS uses the five axially located fixed in-core instrumentation system, the fifth-order Fourier series technique was chosen to appropriately determine the Fourier coefficients. In addition, the current COLSS algorithm allows a constant axial buckling in the on-line axial power shape synthesis. It is therefore important to determine the optimal constant axial buckling based on its effect on the COLSS calculations.

2. Description of Axial Power Shape Synthesis

The fifth-order Fourier series technique uses the five modes of sine curves with the Fourier weighting coefficients. The core average axial power shape is constructed based on the trigonometric form by utilizing in-core detector signals :

$$\phi(z) = \sum_{i=1}^{5} A(i) \sin\left(i \pi \frac{z+\delta}{H+2\delta}\right)$$

$$= \sum_{i=1}^{5} A(i) \sin\left(i \pi B \frac{z+\delta}{H}\right) \quad (1)$$

and

$$D(j) = \int_j \phi(z)\, dz \quad , \quad (2)$$

where

$\phi(z)$–Neutron flux at axial location z

A(i)–Fourier weighting coefficients

H–Active core height

δ–Extrapolated length where neutron flux is assumed to be zero

B–Axial buckling

D(j)–Normalized detector signals at level j, % of core power

The axial buckling (B) is defined as follows.

$$B \equiv \frac{H}{H+2\delta} \quad (3)$$

Substitute Eq.(1) into Eq.(2)

$$D(j) = \sum_{i=1}^{5} A(i) \int_j \sin\left(i \pi B \frac{z+\delta}{H}\right) dz \quad (4)$$

Let

$$H(i,j) = \int_j \sin\left(i \pi B \frac{z+\delta}{H}\right) dz \quad (5)$$

Then, Eq.(4) becomes

$$D(j) = \sum_{i=1}^{5} H(j,i)\, A(i) \quad (6)$$

Rewrite Eq.(6) in matrix form,

$$\mathbf{D} = \mathbf{H}\,\mathbf{A} \tag{7}$$

The Fourier series coefficients vector, **A**, is then determined as below:

$$\mathbf{A} = \mathbf{H}^{-1}\,\mathbf{D} \tag{8}$$

From Eq.(1), the axial power shape can be constructed by forming the product of the Fourier series matrix **SPLIN** and the Fourier series coefficient vector **A**.

$$\mathbf{APKD} = \mathbf{SPLIN}\,\mathbf{A}\ , \tag{9}$$

where

APKD–Vector of node axial powers

SPLIN–Fourier series matrix

The above two matrices, $\mathbf{H}^{-1}$ and **SPLIN**, are the prestored constants in COLSS database which were determined based on the optimal constant axial buckling.

3. Results and Discussions

The four sets of the two matrices, $\mathbf{H}^{-1}$ and **SPLIN**, were generated depending on the assumed value of the axial buckling (B). This paper examined the four cases (B=0.75, 0.8, 0.9 and 1.0) for typical axial power shapes, i.e., center–peak, saddle–type and flat–type which would occur at beginning of cycle (BOC), middle of cycle (MOC) and end of cycle (EOC) in sequence. In addition, the skewed axial power shape is also studied. The $\mathbf{H}^{-1}$ and **SPLIN** sets were then used to construct the 20–node core average axial power shape which was thereafter used in the COLSS calculations of typical net margins of LHR and DNBR alarms.

The error between the best estimate and the COLSS axial power shape is defined as

Table 1. Results of Axial Buckling Variation

Case #	Power Shape	B	RMSError(%) 20-node	RMSError(%) 16-node	Net Margin to LHR Alarm(1)	Net Margin to DNBR Alarm(1)
1	Center-Peak	0.75	11.3	2.1	116.4	111.6
2	(BOC)	0.8	10.5	2.0	116.3	111.6
3		0.9	4.5	0.8	116.2	111.5
4		1.0	13.7	3.9	116.0	111.0
5	Saddle-Type	0.75	15.8	4.3	124.6	106.4
6	(MOC)	0.8	13.1	3.4	124.7	106.4
7		0.9	4.0	1.5	125.3	106.9
8		1.0	17.1	9.3	122.9	105.9
9	Flat-Type	0.75	8.5	2.0	138.1	118.6
10	(EOC)	0.8	6.1	1.4	137.7	118.6
11		0.9	4.1	3.8	135.5	119.1
12		1.0	21.1	12.6	119.4	117.8
13	Skewed	0.75	4.6	2.8	111.9	104.6
14	Shape	0.8	4.4	2.7	111.8	104.5
15		0.9	2.1	1.7	111.9	104.2
16		1.0	5.9	3.7	112.4	102.0

Note : (1) The typical values (in % of rated power) which were calculated based on the preliminary information for YGN 3&4.

$$E_i = \frac{Fz(i)_{COLSS} - Fz(i)_{B.E.}}{Fz(i)_{B.E.}} \times 100 \qquad (10)$$

where

Fz(i)–Normalized axial power at node i (i=1, 2, ···, N)

N–Number of axial nodes

The roo–mean–square (RMS) error is then calculated by

$$RMS = \sqrt{\frac{\sum_{i=1}^{N} E_i^2}{N}} \qquad (11)$$

COLSS currently calculates the core axial power shape at 20 nodes. It is general to check the RMS error based on the 20–node axial powers. However, the 16–node based RMS error (excluding 10% of core bottom and top region) was also evaluated in this paper because the uncertainty in the core end region is generally large. Table 1 shows the root–mean–square (RMS) error of typical core average axial power shapes and the net margins to both LHR and DNBR alarms for YGN 3&4. The overall uncertainties associated with both LHR and DNBR were incorporated in the net margins. It must be noted that the net margins in Table 1 are typical values which were clculated based on the preliminary information for YGN 3&4. The selection of the optimal constant axial buckling should be made to give the maximum limiting net margin and the comparable RMS errors for the various axial power shapes.

The case of B=0.9 gave the least RMS error regardless of the axial power shape types except the 16–node based RMS error for flat–type shape. The case of B=0.9 also gave the biggest limiting net margin to DNBR alarm (case #7) and the comparable limiting net margin to LHR alarm (case #3).

Figure 2 through Figure 5 show the comparison of typical axial power shapes with respect to the best estimate (B.E.) results which were generated by the best estimate neutronics compuer code [4]. All cases except the case of B=1.0 agree well with the B.E. center–peak axial power shape (Fig. 2). The case of B=0.9 shows the best agreement while the cases of B=0.75 and B=0.8 show a slight disagreement for saddle–type power shape (Fig. 3). The case of B=0.8 agrees with the best estimate shape better than other cases except at the first and the last nodes for flat–type power shape (Fig. 4). This is the reason for bigger 20–node based RMS error but smaller 16–node based RMS error for flat–type shape (case #10 in Table 1). For top–skewed axial power shape (Fig. 5), all of the examined cases except B=1.0 show good agreement with the B.E. results.

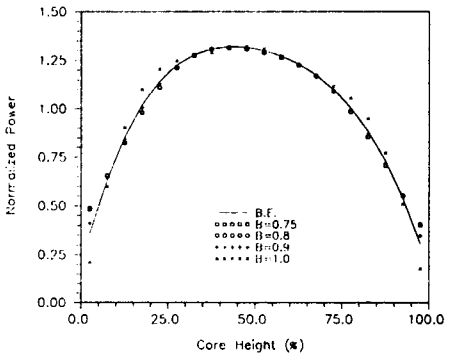

Fig. 2. Comparison of Center–Peak Axial Power Shape

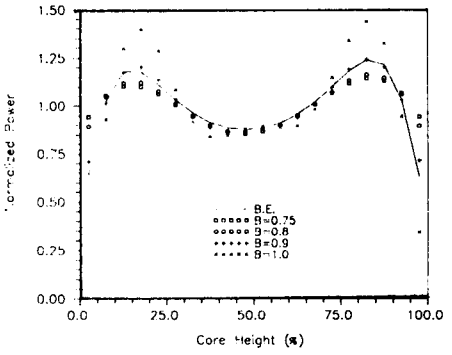

Fig. 3. Comparison of Saddle–Type Axial Power Shape

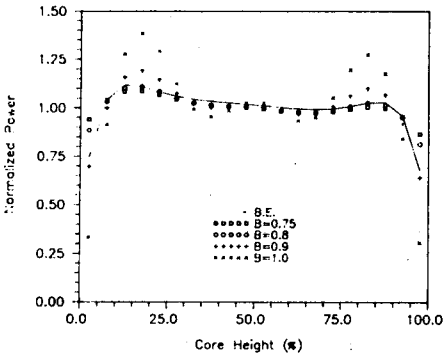

Fig. 4. Comparison of Flat-Type Axial Power Shape

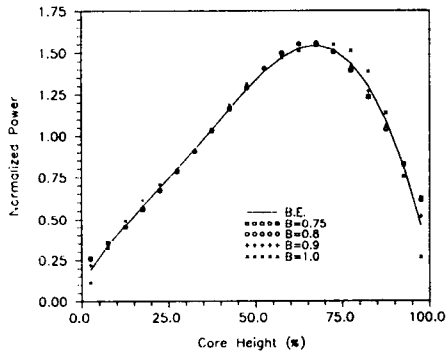

Fig. 5. Comparison of Top-Skewed Axial Power Shape

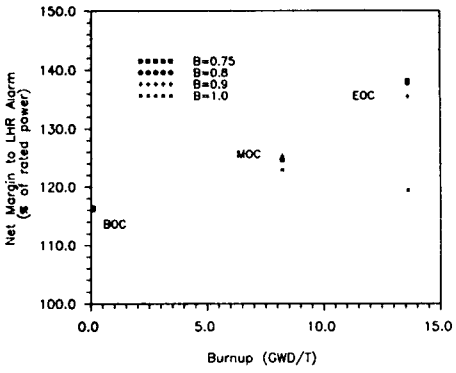

Fig. 6. Variation of Net Margin to LHR Alarm

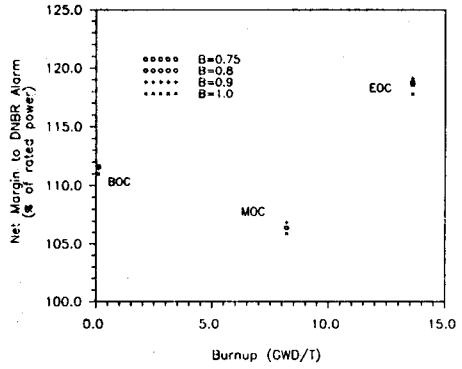

Fig. 7. Variation of Net Margin to DNBR Alarm

Figure 6 and Figure 7 show the distributions of the typical net margins to LHR alarm and DNBR alarm. The case of B=0.9 gave the biggest margin to DNBR alarm for saddle-type and flat-type shapes, and a little bigger margin to LHR alarm for saddle-type shape than other cases but smaller margin to LHR alarm for flat-type shape (cases # 7, #11 in Table 1) than the cases of B=0.75 and 0.8. There is no significant difference in margins to both LHR and DNBR alarms for center-peak shape (cases #1-#4 in Table 1).

In summary, the results in the case of B=0.9 give the maximum limiting net margin (case #11 in Table 1) and the least 20-node based RMS errors. It is therefore believed that the constant axial buckling of 0.9 is optimal value. In addition, the above results show the dependence of optimal axial buckling on axial power shape. However, the constant axial buckling is currently used in the current on-line axial power shape synthesis due to its simplicity and fast computation. Since the upgraded plant computer system enhanced the capacity of the on-line calculations, the axial buckling as a function of axial power shape could be considered in the future.

4. Conclusions

From the above results, the following conclusions can be deduced : (1) the case of B=0.9 is the optimal choice of the constant axial buckling for the fifth–order Fourier series technique in current COLSS, and (2) the axial buckling as a function of axial power shape could be considered in COLSS to increase the operating margin in the future.

References

1. M.L. James, G.M. Smith, J.C. Wolford, "Applied Numberical Methods for Digital Computation with FORTRAN and CSMP," Second Edition 1977, Harper & Row, Publishers Inc..
2. Combustion Engineering Inc., "Overiew Description of the Core Operating Limit Supervisory System," CEN–312–P, Revision 01–P, November 1986.
3. Korea Electric Power Corporation, "Yonggwang Units 3&4 Preliminary Safety Analysis Report," Vol.10(Ch.16), 1988.
4. Combustion Engineering Inc., "User's Manual for FLAIR," CE–CES–99 Rev.0–P, July 1988.